15 October 1999

ELSEVIER

Chemical Physics Letters 312 (1999) 37–44

CHEMICAL PHYSICS LETTERS

www.elsevier.nl/locate/cplett

Mechanism for the reaction of hydroxyl radicals with dimethyl disulfide

N.I. Butkovskaya [a], D.W. Setser [b,*]

[a] *Institute of Chemical Physics, Russian Academy of Sciences, 117334 Moscow, Russian Federation*
[b] *Kansas State University, Department of Chemistry, Manhattan, KS, 66506, USA*

Received 10 May 1999; in final form 14 July 1999

Abstract

Strong infrared chemiluminescence from the reactions of OH and OD radicals with CH_3SSCH_3 was observed in a discharge flow reactor viewed by a Fourier transform spectrometer. The recorded spectra were identical to the H_2O and HDO plus D_2O emission spectra from the $OH + CH_3SH$ and $OD + CH_3SD$ reactions, respectively. These observations strongly suggest that the primary reaction in the OH and $OD + CH_3SSCH_3$ system generates CH_3SH and CH_3SD molecules with the observed emission arising from the $OH + CH_3SH$ and $OD + CH_3SD$ secondary reactions.

1. Introduction

Dimethyl disulfide (CH_3SSCH_3, abbreviated as DMDS) is one of the naturally occurring sulfur compounds that plays an important role in atmospheric chemistry. The oxidation in the troposphere is mainly initiated by reaction with OH radicals and the final products depend on subsequent elementary steps involving the radicals [1–4] produced in the primary step. Studies of the reaction of CH_3SSCH_3 with OH were reviewed by Tyndall and Ravishankara [2], and the recommended value of the rate coefficient at 298 K is $k_1 = (2.0 \pm 0.3) \times 10^{-10}$ cm^3 molecule^{-1} s^{-1}. Wine et al. [4] found a negative temperature dependence in the 244–367 K range and suggested that addition to DMDS was the first step of the reaction with rapid decomposition to $CH_3S + CH_3SOH$ as the likely fate of the adduct.

$$OH + CH_3SSCH_3 \rightarrow CH_3S(OH)SCH_3 \rightarrow CH_3SOH + CH_3S \quad (1a)$$

The final products of the OH + DMDS reaction in an air + NO atmosphere [5] also have been interpreted in terms of (1a). Later, Domine and Ravishankara [6,7] using laser-induced fluorescence and photoionization mass-spectrometry observed both CH_3S and CH_3SOH as products of the OH + DMDS reaction system. However, the measured CH_3S yield was only $28 \pm 20\%$ and the CH_3SOH yield was not quantified [6]. The rate constant of the $OH + CH_3SCH_3$ reaction, which proceeds only by abstraction for our low pressure experimental conditions [8], is nearly two orders of magnitude smaller, $(4.4 \pm 0.3) \times 10^{-12}$ cm^3 molecule^{-1} s^{-1} [2], than k_1, which is strong evidence that the $OH + CH_3SSCH_3$ reac-

* Corresponding author. Fax: +1-785-532-6666; e-mail: setserdw@ksu.edu

0009-2614/99/$ - see front matter
PII: S0009-2614(99)00862-3

tion proceeds by a mechanism other than abstraction of a hydrogen atom. Based on the above-mentioned results, the addition–decomposition mechanism (1a) has been accepted for modeling the DMDS oxidation under atmospheric conditions [3,9].

The reaction of OH with methanethiol, another atmospherically important sulfur compound, has a large rate constant, $33 \pm 4 \times 10^{-12}$ cm^3 molecule^{-1} s^{-1}, and it mainly proceeds through addition of OH to the sulfur atom followed by the elimination of H_2O [2,8]:

$$OH + CH_3SH \rightarrow CH_3S(OH)H \rightarrow CH_3S + H_2O \quad (2a)$$

$$OH + CH_3SH \rightarrow CH_2SH + H_2O \quad (2b)$$

The dominant role of (2a) was confirmed in our recent studies of the reactions of methanethiol with OH and OD radicals using a discharge flow reactor with a Fourier-transfer infrared (IR) spectrometer [8,10] to observe the water products. The available energy of (2a), 34.4 kcal mol^{-1}, is sufficient to excite up to three stretching quanta in the water molecule; the vibrational distributions of H_2O and HDO from reaction (2) were characteristic for an addition–elimination reaction and differed substantially from the distribution from the OH(OD) + $(CH_3)_2S$ reaction, which proceeds by abstraction. Examination of the analogous reaction with CH_3SD, where channels (a) and (b) give distinguishable products,

$$OD + CH_3SD \rightarrow CH_3S + D_2O \quad (3a)$$

$$OD + CH_3SD \rightarrow CH_2SD + HOD \quad (3b)$$

revealed that (3b) cannot be entirely neglected, since both D_2O and HOD were observed [10], but the ratio of the channels (0.16 ± 0.05) is roughly in proportion to the rate constant (per H atom) for abstraction from $(CH_3)_2S$ versus the rate constant for reaction (2).

As part of our comprehensive study [8,10–13] of OH reactions with various molecules using the IR chemiluminescence experimental technique, we obtained the rather unexpected result that the observed spectra from OH + DMDS were identical to the spectra from OH + CH_3SH and the spectra from OD + DMDS were identical to that from OD + CH_3SD. This observation implies that the DMDS · OH adduct partly decomposes with formation of a CH_3SH molecule that subsequently reacts with OH radical to give the observed H_2O chemiluminescence.

$$OH + CH_3SSCH_3 \rightarrow CH_3S(OH)SCH_3 \rightarrow CH_3SO + CH_3SH \quad (1b)$$

In addition to the similarity of the spectra, the dependencies of the HOD and D_2O integrated emission intensities upon reagent concentrations for OD + DMDS reaction were compared with the HOD emission intensity from OD + H_2S reaction to support the proposed mechanism. The very large rate constant for (1) plus the sizeable rate constant for (2) or (3) enables the IR emission from water molecules to be observed.

2. Experimental method

The experiments were done in the KSU laboratory employing methods described in previous papers [8,10–13]. The IR chemiluminescence from vibrationally excited products was recorded by a Fourier-transform IR spectrometer (BIORAD), which viewed the emission from a fast-flow chemical reactor (40 mm ID Pyrex glass pipe) through a NaCl window. Each measured spectrum represents an average of 512 scans of the spectrometer operated with a spectral resolution of 2 cm^{-1}. The OH or OD radicals were produced via the reaction of H or D with NO_2 in the pre-reactor section of the flow reactor. The H or D atoms were generated by a microwave discharge through $H_2(D_2)$/Ar mixtures. The DMDS, CH_3SH or H_2S reactants were introduced into the center of the linear reactor through a ring injector located 20 cm downstream of the hydrogen and nitrogen dioxide inlets and 3.5 cm upstream of the center of the NaCl observation window. The total pressure in the reactor was 0.5 torr, the flow velocity was about 130 m s^{-1}, corresponding to a reaction time between OH(OD) and DMDS of $\Delta t \sim 0.25$ ms. The concentration of H or D atoms was about 2×10^{13} molecule cm^{-3}; the NO_2 concentration was about 1×10^{14} molecule cm^{-3}; the reactant concentrations were varied from 3.1×10^{11} to 1.1×10^{13} molecule cm^{-3}. Commercial tank grade Ar passed

through three molecular sieve traps cooled by acetone/dry ice mixture and liquid N_2 before being added to the reactor. These traps reduce the H_2O and CO_2 impurities. The isotopic and chemical purity of CH_3SD (CDN Isotopes) were $>94\%$ and $>99.6\%$, respectively. The CH_3SSCH_3 (purchased as a liquid from Aldrich Chemical, 99%) was degassed in freeze–thaw–pump cycles. The central fraction from a room temperature liquid sample was expanded into a 10 l Pyrex glass bulb and a 7% mixture in Ar was prepared. This mixture was used during the same working day. The DMDS mixture was metered to the reactor through a 10 mm ID glass line approximately 50 cm in length. Experiments were done with two independently prepared DMDS/Ar mixtures.

The computer simulation procedure used to assign stretching and bending mode distributions from the H_2O, HOD and D_2O spectra has been described [8,10–13]. In the present work, our interpretations are mainly based on the overall appearance of the emission spectra and on the total emission intensities, and we will not describe the simulation procedures. The limited degree of vibrational relaxation of the product water molecules for the short reaction time and low Ar pressure has been discussed in Refs. [8,10–13]. For the conditions of the experiments to be described, the populations in the ν_1 and ν_3 modes of H_2O and D_2O and the populations in the ν_1 and ν_2 modes of HOD are coupled by collisions with Ar. The vibrational relaxation of H_2O, D_2O, and HOD molecules beyond this coupling is negligible. The only assumption in the spectral simulation is that the rotational distributions are represented by 300 K Boltzmann distributions.

3. Results and discussion

3.1. Chemiluminescent spectra

The raw chemiluminescent spectra from the OH + DMDS and OD + DMDS reaction systems are shown in Fig. 1b,d, respectively. They can be compared to the H_2O spectra in the 3200–4000 cm^{-1} range from the OH + CH_3SH reaction (Fig. 1a) and D_2O (2400–3000 cm^{-1}) and HOD (3200–4000 cm^{-1}) spectra from the OD + CH_3SD reaction (Fig. 1c) measured in our previous studies [8,10]. Spectra were selected for comparison that had similar reagent concentrations (see the figure caption), and the relative intensities in Fig. 1 reflect the relative concentrations of the isotopic water molecules generated by the CH_3SH (CH_3SD) and DMDS chemical reaction systems. One should note the comparable yields of water molecules in both systems. The observation of D_2O emission spectra from OD + DMDS is convincing evidence for the importance of reaction (1b). The observation of D_2O emission from the OD + DMDS reaction also eliminates the possibility that the decomposition of DMDS in the gas handling procedure could be the source of the water emission, e.g., the source cannot be OD + CH_3SH.

The spectra from the DMDS and CH_3SH (CH_3SD) systems are very similar. Analysis of the spectra by computer simulation showed only very small differences, which can be explained from contamination in the OD + CH_3SD system by the CH_3SH isotopic impurity [10]. The H_2O stretching distributions obtained by simulation of the spectra are $P_{1,3}(1{:}2{:}3) = 66{:}30{:}5$ from DMDS and $P_{1,3}(1{:}2{:}3) = 68{:}26{:}6$ from CH_3SH; the D_2O stretching distributions are $P_{1,3}(1{:}2{:}3) = 64{:}33{:}2$ for DMDS and $P_{1,3}(1{:}2{:}3) = 65{:}32{:}3$ for CH_3SD. The 1,3 subscripts denote the coupled ν_1 and ν_3 modes. The HOD emission in the 3200–4000 cm^{-1} range is overlapped with the $\upsilon_2 + \upsilon_3$ combination bands from D_2O, and a complete analysis of these spectra will be made later [10]. It is sufficient here to note that the two spectra in Fig. 1c,d in the 3200–4000 cm^{-1} range are identical. The spectral pattern from the OD + DMDS system, including the intensity ratio between the D_2O and HOD parts of the spectra, did not change with variation of DMDS or OD concentration, when the former was varied between 1 and 7×10^{12} molecule cm^{-3} and the latter was varied between 1.5 and 2.8×10^{13} molecule cm^{-3}. The D_2O and HOD emission arise from the same source in the OD + DMDS reaction and, in fact, this source is the reaction of OD with CH_3SD.

3.2. Kinetic behavior and reaction mechanism

Comparative kinetic measurements were carried out for the OD + DMDS and OD + H_2S systems in order to quantify the water yield in the DMDS system. The H_2S system was chosen as one nearly

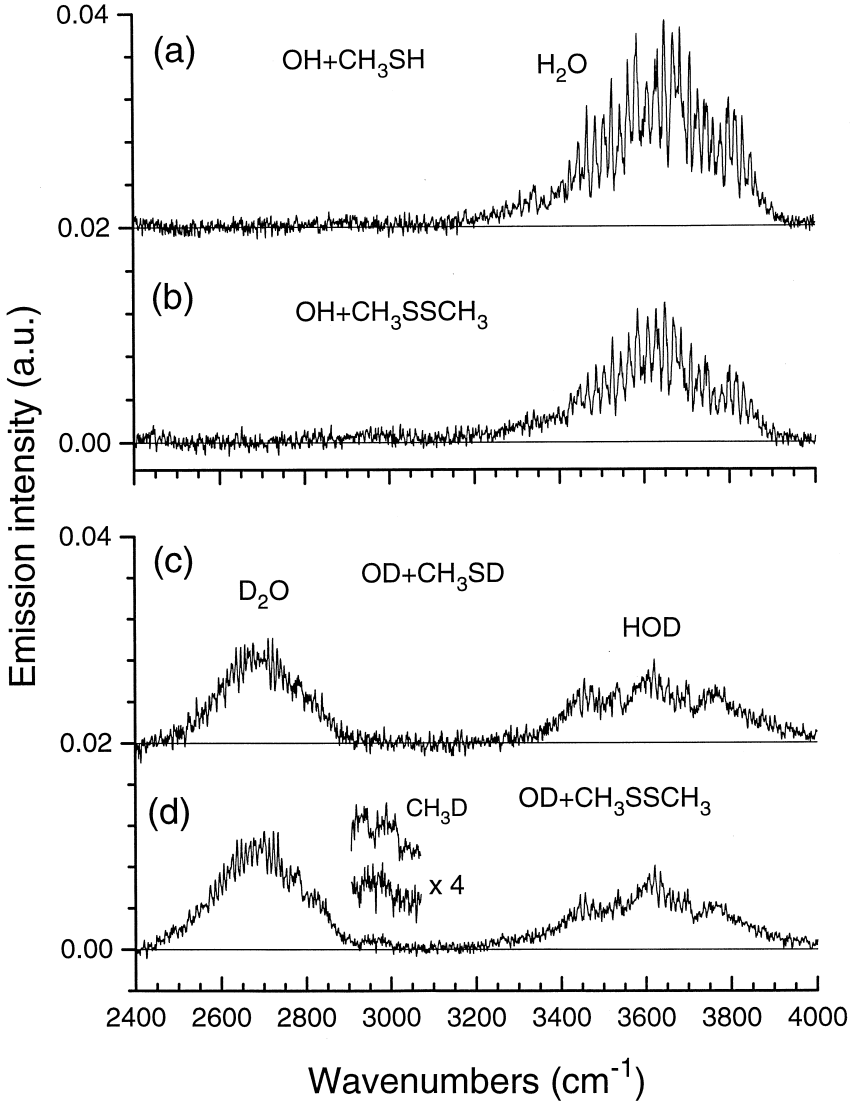

Fig. 1. Raw chemiluminescent spectra obtained at 0.5 torr and $\Delta t = 0.25$ ms; the spectra for (a) and (c) have been elevated so that 0.02 is their base line. (a) $OH + CH_3SH$ system, $[OH] = 2.1 \times 10^{13}$, $[NO_2] = 1.6 \times 10^{14}$ and $[CH_3SH] = 7.1 \times 10^{12}$ molecules cm^{-3}. (b) OH + DMDS system, $[OH] = 2.1 \times 10^{13}$, $[NO_2] = 6.1 \times 10^{13}$ and DMDS $= 7.0 \times 10^{12}$ molecules cm^{-3}. (c) $OD + CH_3SD$ system, $[OD] = 2.7 \times 10^{13}$, $[NO_2] = 1.0 \times 10^{14}$ and $[CH_3SD] = 1.2 \times 10^{13}$ molecules cm^{-3}. (d) OD + DMDS system, $[OD] = 2.8 \times 10^{13}$, $[NO_2] = 1.5 \times 10^{14}$ and $[DMDS] = 1.1 \times 10^{13}$ molecules cm^{-3}.

free of secondary chemistry [8]. The spectra were corrected for the detector response function and the total intensity was measured in the 2400–3050 cm^{-1} (D_2O) and in the 3200–4000 cm^{-1} (HOD) spectral ranges. The dependence of the D_2O and HOD integrated emission intensities on DMDS and H_2S concentration are shown in Fig. 2a. The HOD emission intensity (closed squares and dashed line) from the H_2S reaction with rate coefficient $k = 4.7 \times 10^{-12}$ cm^3 $molecule^{-1}$ s^{-1} [11] shows a linear dependence on H_2S concentration, as expected. These intensities were converted to relative concentrations (open squares) using the Einstein coefficients and the vibrational distribution. The plots with solid triangles

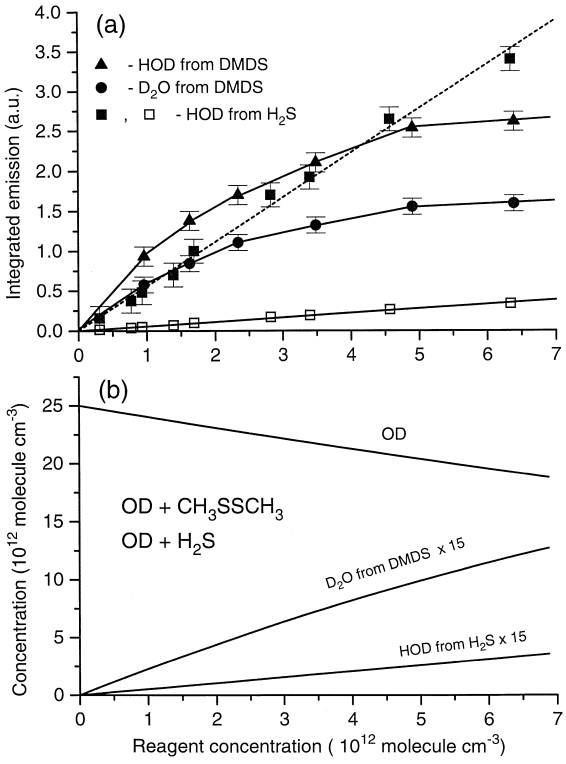

Fig. 2. Plots of integrated product emission intensities against reagent concentration: (a) HOD and D_2O versus [DMDS] from OD + DMDS and HOD versus $[H_2S]$ from OD + H_2S at 0.5 torr ($\Delta t = 0.25$ ms) with $[NO_2] = 8.2 \times 10^{13}$ and $[OD] = 2.5 \times 10^{13}$ molecule cm^{-3}. The solid squares connected by the dotted line are the actual integrated HOD intensities from OD + H_2S; the open squares connected by the solid line are the HOD intensities scaled by the Einstein coefficients to represent relative HOD concentrations. The solid triangles and circles connected by solid curves are the HOD and D_2O concentrations from DMDS that were obtained from the intensities after adjustment for Einstein coefficients. (b) Calculated product concentrations for the conditions of (d) and the reaction scheme from Section 3.2 with the rate constants quoted in the text.

and solid circles from DMDS were obtained by adjustment of the intensities for the Einstein coefficients of the D_2O and HOD transitions [8,10] to obtain relative concentrations. The plot for DMDS measured at 0.5 torr ($\Delta t = 0.25$ ms) displays some curvature. Roughly, we can interpret the plot as a linear growth below 3×10^{12} molecule cm^{-3} and a fall off due to the [OH] consumption at higher DMDS concentrations. The experimental (Fig. 1a) and calculated (Fig. 2b) relative concentrations from OD + H_2S and OD + DMDS for the proposed mechanism are in satisfactory agreement.

The kinetic behavior for OD + DMDS requires a reaction scheme in which D_2O and HOD are both formed by the same secondary reaction involving OD radicals. We consider the following possible mechanisms:

1. The initial step yields methanethiol (reaction (1b)), which leads to production of water via (3).
2. Hydroxyl radicals react directly with the DMDS · OD adduct either giving methanethiol, which subsequently reacts with OD,

$$OD + CH_3SS(OD)CH_3 \rightarrow 2CH_3SD + O_2 \quad (4a)$$

or giving water via reactions (4b) and (4c).

$$OD + CH_3SS(OD)CH_3 \rightarrow CH_3SS(O)CH_3 + D_2O \quad (4b)$$

$$OD + CH_3SS(OD)CH_3 \rightarrow CH_2SS(OD)CH_3 + HOD \quad (4c)$$

3. The primary reaction occurs with formation of CH_3S and CH_3SOD, as in (1a), and water molecules are produced by subsequent reaction of hydroxyl radicals with methanesulfenic acid.

$$OD + CH_3SOD \rightarrow CH_3SO + D_2O \quad (5a)$$

$$OD + CH_3SOD \rightarrow CH_2SOD + HOD \quad (5b)$$

To give a spectrum similar to that from reaction (3), alternative reaction(s) must fulfill two conditions: (i) the absolute yield and branching ratio between D_2O and HOD producing channels must be equal to those for channels (3a) and (3b), and (ii) the energetics and, moreover, the dynamics of the hydrogen transfer in both channels must be very similar, so as to give similar vibrational distributions for both D_2O and HOD. Therefore, the enthalpy changes for the secondary reaction should be close to those for reaction (3) with $\Delta_r H_0^\circ(3a) = -32.0$ kcal mol^{-1} and $\Delta_r H_0^\circ(3b) = -25.7$ kcal mol^{-1}.

Reaction (4a) can be removed from consideration, as in this case reaction (3) would be a tertiary reaction, and even if the secondary reaction (4a) is as fast as reaction (1), the water yields would be an order of magnitude less than from (1b) + (3) and the emission could be observed only at substantially higher OD and DMDS concentrations. The direct

production of water from the adduct can be ruled out because formation of HOD via the H atom abstraction from the methyl group should have a negligible rate. It is doubtful that reaction (4b) is sufficiently exothermic to give D_2O with the necessary energy.

Although reaction (5) has never been observed, it is likely to occur [9]. We failed to find experimental thermochemical data for CH_3SOH or CH_3SO; however, the equilibrium structure and $\Delta_f H_{298}°(CH_3SOH) = -33.9$ kcal mol^{-1}, was calculated in an ab initio study of the $(CH_3)_2S + OH$ reaction at the G2(MP2) level of theory [14]. Turecek also calculated $\Delta_r H_{298}°(5a) = -51.7$ kcal mol^{-1} and $\Delta_r H_{298}°(5b) \approx -25.8$ kcal mol^{-1}, from which the $\Delta_f H_0°(CH_3SO)$ was estimated as -18.5 kcal mol^{-1}. Comparing reactions (5) and (3), we see that abstraction from the C–H bonds releases similar amounts of energy, but channel (5a) is much more exothermic than channel (3a). In other words, the C–H bond energies are very close, 95.0 [14] and 93.9 kcal mol^{-1} [15], but $D(CH_3SO–H) = 68.8$ kcal mol^{-1} is nearly 20 kcal mol^{-1} weaker than $D(CH_3S–H) = 87.4$ kcal mol^{-1}. An even smaller value, $D(CH_3SO–H) = 59$ kcal mol^{-1}, was assigned by Yin et al. [9] from consideration of the O–H bond energy trend in the $HOS(O)_xO–H$ and $CH_3S(O)_xO–H$ series. Undoubtedly, the weak O–H bond in CH_3SOH would lead to a shift of branching ratio, as well as to a higher vibrational excitation of the product water molecule in channel (5b) compared to (3b), which is contrary to the experimental observation. Mechanism (1b) followed by (3) seems the most plausible scenario. As a further test, the D_2O production by sequential reactions (1b) and (3a) are compared with the HOD production from $OD + H_2S$ in Fig. 2b. The calculation corresponds to $[NO_2]_0 = 8.2 \times 10^{13}$ and $[OD]_0 = 2.5 \times 10^{13}$ molecule cm^{-3}. The consumption of DMDS was about 70% for an initial $[DMDS]_0 = 7.0 \times 10^{12}$ molecule cm^{-3}. The observed and calculated relative D_2O and HOD yields are in satisfactory agreement.

Using the calculated $\Delta_f H_{298}°(CH_3SOH)$ value together with $\Delta_f H_{298}°(OH) = 9.3$, $\Delta_f H_{298}°(CH_3SSCH_3) = -5.8$ kcal mol^{-1} and $\Delta_f H_{298}°(CH_3S) = (33.2)$ kcal mol^{-1} [11], the enthalpy change for reaction (1a) is -4 kcal mol^{-1}. As the accuracy of the $\Delta_f H_{298}°$ values for CH_3S and CH_3SOH are not high, reaction (1a) can be considered as nearly thermoneutral. The enthalpy of reaction (1b) is -28 kcal mol^{-1} for $\Delta_f H_{298}°(CH_3SO) = -18.5$ kcal mol^{-1}, and reaction (1b) is more exothermic than reaction (1a).

Secondary reactions in our reactor also could include $NO_2 + CH_3S$ and CH_3SO [13], and the tertiary OD reactions also need to be considered.

$$CH_3S + OD \rightarrow CH_3SOD \rightarrow CH_3SO + D \quad (6a)$$

$$CH_3S + OD \rightarrow CH_3SOD \rightarrow CH_3D + SO \quad (6b)$$

$$CH_3SO + OD \rightarrow CH_3S(O)OD \rightarrow CH_3D + SO_2 \quad (7)$$

Reactions (6) and (7) have not been observed, but their rate constants should be large; $\Delta_r H_{298}°(6a) = -8.7$, $\Delta_r H_{298}°(6b) = -58.9$ and $\Delta_r H_{298}°(7) = -79.7$ kcal mol^{-1} and high vibrational excitation of the products is likely. Reactions (6) and (7) are mentioned because of the weak chemiluminescence observed in the 2900–3050 cm^{-1} range. An enlarged spectrum in this range is shown in Fig. 1d, where its shape is compared with CH_3D emission from the unimolecular decomposition of $CH_3C(O)D \rightarrow CH_3D + CO$ [1]. Although too weak to be assigned with certainty, this emission may be a progression of red shifted Q-branches of the CH_3D triply degenerate vibration of the ν_4 mode centered at 3000 cm^{-1}.

3.3. Comparison with previous studies

The CH_3S radical [6,7] was detected via laser-induced fluorescence as a product of reaction (1) and the yield was reported as $28 \pm 20\%$. Since the direct detection of CH_3S was made for conditions such that [DMDS] > [OH], the LIF data and our work suggest that the branching to (1a) is definitely less than to (1b). The detection of CH_3SOH at m/e 64, CH_3SO at m/e 63 and CH_3SH at m/e 48 by photoionization mass spectrometry in a flow reactor was also reported in that study. Since the signals were not quantified, the relative concentrations are uncertain.

[1] Vibrational excitation of CH_4 and CH_3D molecules was observed from the unimolecular decomposition of chemically activated $CH_3C(O)H$ or $CH_3C(O)D$ and $CH_3C(O)OH$ or $CH_2DC(O)OH$ obtained from successive $CH_3C(O)I + H$(or D) and $ICH_3C(O)OH + H$(or D) reactions, respectively (see Ref. [16]).

Observation of CH_3SO and CH_3SH is consistent with (1b). Comparison of the temporal profiles of the CH_3SOH, CH_3SO and CH_3S signals suggests that all can be primary products; the CH_3SH profile was not presented in the article. It seems that the data of Ref. [6] are compatible with our IR measurements, if the branching ratio of (1a) to (1b) is $\lesssim 1/3$.

The products from reaction (1) are important for modeling the oxidation mechanism in the atmosphere, especially the production of sulfuric acid versus methanesulfonic acid, CH_3SO_3H (17). According to current views, a simplified mechanism of the oxidation of DMDS (or any sulfur containing compound giving CH_3S) in the atmosphere proceeds through the following steps to yield CH_3SO_3H [1]:

$$CH_3S + O_2 \rightarrow CH_3SOO$$

$$CH_3SOO + NO \rightarrow CH_3SO + NO_2$$

$$CH_3SO + O_2 \rightarrow CH_3S(O)OO$$

$$CH_3S(O)OO + NO \rightarrow CH_3SO_2 + NO_2 \qquad (8)$$

$$CH_3SO_2 + O_2 \rightarrow CH_3S(O)_2OO$$

$$CH_3S(O)_2OO + NO \rightarrow CH_3SO_3 + NO_2$$

$$CH_3SO_3 + RH \rightarrow CH_3SO_3H + R$$

The alternative product, H_2SO_4, requires formation of SO_2 as the intermediate product. One possible channel is collisional decomposition of CH_3SO_2 to give $CH_3 + SO_2$, which competes with reaction with O_2. Both CH_3SO_3H and SO_2 were found by Hatakeyama and Akimoto [5] for reactions of CH_3SH, DMS and DMDS with OH under atmospheric conditions. In their experiments, OH radicals were generated by the photolysis of alkyl nitrites, RCH_2ONO. The authors invoked reaction (1a) to explain the enhanced yield of CH_3SO_3H from DMDS compared to CH_3SH. Though gas-phase reactions of CH_3SOH have been never observed, it was speculated that the increase of the CH_3SO_3H yield arose from the direct association reaction

$$CH_3SOH + O_2 + M \rightarrow CH_3SO_3H + M \qquad (9)$$

However, reaction (9) seems rather improbable as an elementary reaction, and the increase of CH_3SO_3H yield can be explained by the formation of CH_3SO in (1b).

In the FTIR study of the photolysis of DMDS at 760 torr in an $(O_2 + N_2)$ mixture, Barnes et al. [3] found that the CH_3SO_3H formation increased with an increase of the concentration of OH radicals. As a possible explanation, formation of CH_3SO_3H in reaction (10)

$$CH_3SOH + CH_3SO_3 \rightarrow CH_3SO + CH_3SO_3H \qquad (10)$$

was proposed. However, the same arguments are valid for the alternative products, CH_3SH and CH_3SO, owing to the possibility of reaction (11).

$$CH_3SH + CH_3SO_3 \rightarrow CH_3S + CH_3SO_3H \qquad (11)$$

4. Conclusions

The IR emission spectra from the $OH + CH_3SSCH_3$ and $OD + CH_3SSCH_3$ reactions were observed from a fast flow reactor operating with 0.5 torr of Ar carrier gas. The observed spectra were nearly identical to the spectra obtained from the $OH + CH_3SH$ and $OD + CH_3SD$ reactions. Especially striking is the fact that the products from the $OD + CH_3SSCH_3$ reaction are D_2O and HOD in the same proportion and with the same vibrational distribution as for $OD + CH_3SD$. Comparison of the integrated emission intensities of the $OH(OD) + CH_3SSCH_3$ reaction to those from $OH(OD) + H_2S$ and CH_3SH or CH_3SD shows that the observed intensities from CH_3SCH_3 are consistent with the very fast primary reaction giving CH_3SH (or CH_3SD) + CH_3SO followed by reaction of OH(OD) with CH_3SH (CH_3SD). Comparison of our results with other studies in the literature suggests that the primary reaction has a branching ratio of $\gtrsim 3$ in favor of $CH_3SH + CH_3SO$ versus $CH_3S + CH_3SOH$. The DMDS reaction mainly proceeds via addition of hydroxyl radical to one of the sulfur atoms, followed by four-centered migration of a H atom to the other sulfur atom, which is favored because the S–H bond is stronger than the O–H bond, followed by scission of the S–S bond.

Acknowledgements

The work at Kansas State University was supported by the National Science Foundation Grant CHE-9505032.

References

[1] S.B. Barone, A.A. Turnipseed, A.R. Ravishankara, Faraday Discuss. Chem. Soc. 100 (1995) 39.
[2] G.S. Tyndall, A.R. Ravishankara, Int. J. Chem. Kinet. 23 (1991) 483.
[3] I. Barnes, K.H. Becker, N. Mihalopoulos, in: G. Restelli, G. Angeletti (Eds.), Dimethylsulfide: Oceans, Atmosphere and Climate, CEC, Kluwer Academic Publishers, Netherlands, 1993, p. 197.
[4] P.H. Wine, N.M. Kreutter, C.A. Gump, A.R. Ravishankara, J. Phys. Chem. 85 (1981) 2660.
[5] S. Hatakeyama, H. Akimoto, J. Phys. Chem. 87 (1983) 2387.
[6] F.A. Domine, A.R. Ravishankara, Int. J. Chem. Kinet. 24 (1992) 943.
[7] F.A. Domine, A.R. Ravishankara, C.J. Howard, J. Phys. Chem. 96 (1992) 2171.
[8] N.I. Butkovskaya, D.W. Setser, J. Phys. Chem. A 102 (1998) 6395.
[9] F. Yin, D. Grosjean, J.H. Seinfeld, J. Atmos. Chem. 11 (1990) 309.
[10] N.I. Butkovskaya, D.W. Setser, J. Phys. Chem. A 103 (1999) in press.
[11] N.I. Butkovskaya, D.S. Setser, J. Phys. Chem. A 102 (1998) 9715.
[12] N.I. Butkovskaya, D.W. Setser, J. Chem. Phys. 108 (1998) 2434.
[13] Chemical Kinetics and Photochemical Data for Use in Stratospheric Modeling, NASA JPL Publ. 92-20, 1992.
[14] F. Turecek, J. Phys. Chem. 98 (1994) 3701.
[15] J. Berkowitz, G.B. Ellison, D. Gutman, J. Phys. Chem. 98 (1994) 2744.
[16] N.I. Butovskaya, D.W. Setser, unpublished results.